

High-current H3+ DC beam production with a miniaturized microwave driven ion source at Peking University

Yicheng Dong(董宜承), Shixiang Peng(彭士香), Jianbin Zhu(朱建斌), Bujian Cui(崔步坚), Zhiyu Guo(郭之虞), Jiaer Chen(陈佳洱)

Citation: Chin. Phys. B. 35, 095204 (2026). DOI: 10.1088/1674-1056/ae926d |
CSTR: 32038.14.CPB.ae926d
http://cpb.iphy.ac.cn; http://iopscience.iop.org/cpb

What follows is a list of articles you may be interested in

New progress on DC beam generation: Tens of mA output and 70% fraction from a 2.45 GHz microwave driven ion source

Bujian Cui(崔步坚), Shixiang Peng(彭士香), Jianbin Zhu(朱建斌), Yicheng Dong(董宜承), Zhiyu Guo(郭之虞), Jiaer Chen(陈佳洱)
Chin. Phys. B. 34, 085203 (2025). DOI: 10.1088/1674-1056/adf1ec | CSTR: 32038.14.CPB.adf1ec

Simulation of helium supersonic molecular beam injection in tokamak plasma

Xue-Ke Wu(吴雪科), Zhan-Hui Wang(王占辉), Hui-Dong Li(李会东), Li-Ming Shi(石黎铭), Di Wan(万迪), Qun-Chao Fan(樊群超), Min Xu(许敏)
Chin. Phys. B. 29, 065201 (2020). DOI: 10.1088/1674-1056/ab81fd

Practical 2.45-GHz microwave-driven Cs-free H- ion source developed at Peking University

Tao Zhang(张滔), Shi-Xiang Peng(彭士香), Wen-Bin Wu(武文斌), Hai-Tao Ren(任海涛), Jing-Feng Zhang(张景丰), Jia-Mei Wen(温佳美), Teng-Hao Ma(马腾昊), Yao-Xiang Jiang(蒋耀湘), Jiang Sun(孙江), Zhi-Yu Guo(郭之虞), Jia-Er Chen(陈佳洱)
Chin. Phys. B. 27, 105208 (2018). DOI: 10.1088/1674-1056/27/10/105208

A miniaturized 2.45 GHz ECR ion source at Peking University

Jia-Mei Wen(温佳美), Shi-Xiang Peng(彭士香), Hai-Tao Ren(任海涛), Tao Zhang(张滔), Jing-Feng Zhang(张景丰), Wen-Bin Wu(武文斌), Jiang Sun(孙江), Zhi-Yu Guo(郭之虞), Jia-Er Chen(陈佳洱)
Chin. Phys. B. 27, 055204 (2018). DOI: 10.1088/1674-1056/27/5/055204

New progress on beam availability and reliability of PKU high intensity CW proton ECR ion source

Shi-Xiang Peng(彭士香), Ai-Lin Zhang(张艾霖), Hai-Tao Ren(任海涛), Yuan Xu(徐源), Tao Zhang(张滔), Jing-Feng Zhang(张景丰), Jia-Mei Wen(温佳美), Zhi-Yu Guo(郭之虞), Jia-Er Chen(陈佳洱)
Chin. Phys. B. 26, 025206 (2017). DOI: 10.1088/1674-1056/26/2/025206

RAPID COMMUNICATION

High-current H_3^+ DC beam production with a miniaturized microwave driven ion source at Peking University

Yicheng Dong(董宜承), Shixiang Peng(彭士香)†, Jianbin Zhu(朱建斌), Bujian Cui(崔步坚), Zhiyu Guo(郭之虞), and Jiaer Chen(陈佳洱)

State Key Laboratory of Nuclear Physics and Technology, Peking University, Beijing 100871, *China*

(Received 18 June 2026; revised manuscript received 27 July 2026; accepted manuscript online 30 July 2026)

In recent years, the widespread use of H_3^+ ion beams across various fields, such as high-intensity proton cyclotrons, nuclear physics, astronomy, etc., has created an urgent demand for high-current H_3^+ ion sources. However, ion sources capable of generating direct-current (DC) H_3^+ ion beams of several milliamperes remain scarce to date. Recently, a miniaturized microwave- driven ion source (MMDIS) with a DC 7.6 mA H_3^+ ion beam has been developed at Peking University (PKU), operating at an RF power of only 80 W. Beam analysis indicates that the H_3^+ fraction in the MMDIS extracted beam can reach 68.5%. These results provide a valuable reference for the utilization of H_3^+ beams.

Keywords: H_3^+ ion beam, 2.45 GHz microwave, microwave driven ion source, high current, direct-current (DC) operation

PACS: 52.25.Dg, 52.50.Dg, 52.50.Sw, 52.59.–f

DOI: 10.1088/1674-1056/ae926d **CSTR:** 32038.14.CPB.ae926d

1. Introduction

H_3^+ ion beams have a wide range of applications in accelerators, nuclear physics, astronomy, materials science, etc. In the field of accelerators, the new generation of proton cyclotrons is evolving toward higher beam current, more compact size, and improved efficiency. However, direct proton acceleration is constrained by space-charge effects, resulting in beam quality deterioration.[1–4] For example, the PSI Injector II cyclotron extracts a proton beam of 2.2 mA, making it the highest proton current cyclotron in the world, although space-charge effects also exist.[5] The method of generating high power proton beams by stripping H^- or H_2^+ can mitigate space-charge effects, but they are constrained by the Lorentz dissociation limit, which restricts the increase in beam current and can also lead to problems such as equipment activation, etc.[6–10] H_3^+ ion beams exhibit good resistance to Lorentz dissociation when accelerated to high energies, making them a promising candidate choice for future high-energy, high-intensity proton cyclotrons.[11] In nuclear physics, collision experiments using H_3^+ beams at different energy scales can selectively reveal the physical mechanisms within atomic nuclei.[12] In astrophysics, H_3^+ plays a significant role in cosmic ray detection, interstellar chemistry, and planetary ionospheric observations, owing to its high cosmic abundance and identifiable spectral signatures.[13,14] In material science, H_3^+ ion beams play an important role in the study of material modification and irradiation damage mechanisms.[15] Therefore, the broad applications of H_3^+ have created an urgent demand for high-current H_3^+ ion sources.

H_3^+ ion beams can be generated by a variety of ion sources. In 1959, the Oak Ridge National Laboratory (ORNL) successfully developed a duoplasmatron ion source for accelerators. Owing to its compact structure and high gas utilization efficiency, this ion source became a preferred choice for accelerator applications at the time. It could produce an H_3^+ ion beam of 0.46 mA, with an ion fraction of 15%.[16] Tomsk State University in Russia developed a hollow-cathode Penning ion source. A H_3^+ ion beam of up to several milliamperes in pulse mode could be achieved, with a H_3^+ fraction exceeding 70%.[17] In 2009, Goethe University Frankfurt designed a filament-driven ion source and it successfully generated a DC H_3^+ ion beam of 3.05 mA, with a H_3^+ fraction as high as 95%.[18] These kinds of ion sources can generate H_3^+ ion beams with high fraction, but the beam current is not high enough. ECR ion sources, by virtue of their advantages such as high beam current, low emittance, compact structure, and long lifetime, have become an excellent choice for generating high-current H_3^+ beams. However, there have been virtually no reports on the generation of H_3^+ beams of several milliamperes in DC mode to date. Since 2013, PKU has been engaged in research on ECR hydrogen molecular ion sources. The PMECR II, a hydrogen molecular ion source independently developed by PKU, is capable of delivering a pulsed H_3^+ beam with a current of 20 mA at an extraction voltage of 45 kV. By adjusting the operating parameters, this source can also produce a pulsed H_2^+ beam exceeding 42 mA.[19–21] PKU

†Corresponding author. E-mail: sxpeng@pku.edu.cn

© 2026 Chinese Physical Society and IOP Publishing Ltd. All rights, including for text and data mining, AI training, and similar technologies, are reserved.

has been committed to miniaturizing ion sources while maintaining beam current. In 2018, by overcoming the microwave cutoff limitation, PKU successfully developed a compact microwave driven ion source with a discharge chamber diameter of merely 30 mm. This ion source produced a mixed hydrogen ion beam of 21.7 mA at a DC power of 180 W, demonstrating its excellent performance. By adjusting the operating parameters, this source generated a mixed hydrogen ion beam of 1 mA at a DC power of only 10 W, with an H_3^+ fraction reaching 82%.[22] Later on, this MMDIS generated an H_3^+ beam of 6.2 mA at a DC power of 100 W, with a proportion of 34%.[23] Recently, this MMDIS has successfully produced an H_2^+ beam of 22 mA at a DC microwave power of 150 W, making it the ion source capable of producing the highest H_2^+ beam reported worldwide to date.[24] However, the capability of this ion source to generate DC H_3^+ ion beams has not yet been fully exploited. The mechanism of H_3^+ ion generation and the parameters affecting H_3^+ ion beam current are not yet clear. Recently, a H_3^+ beam of 7.6 mA was obtained at a RF power of only 80 W and the maximum H_3^+ fraction was 68.5% at 50 W, 4×10^{-3} Pa was obtained with this MMDIS. At the same time, the H_2^+ current has been updated to 24 mA with the same source, higher than previous record 22 mA.[24]

This paper proceeds as follows. In Section 2, a global model that elucidates the H_3^+ production mechanism is established, and the MMDIS as well as the experimental test platform are introduced. In Section 3, we present new progress of DC H_3^+ ion beam generation from the MMDIS. In the DC mode, a H_3^+ beam of 7.6 mA was obtained at a RF power of only 80 W, and the maximum H_3^+ fraction was 68.5% at 50 W, 4×10^{-3} Pa. In Section 4, the applications and development prospects of H_3^+ ion sources are discussed.

2. Methodology

2.1. Global model

Achieving a high-current H_3^+ beam requires a thorough understanding of its generation mechanism. Microwave-driven hydrogen plasma contains a variety of species such as hydrogen molecules (H_2), hydrogen atoms (H), protons (H^+), hydrogen molecular ions (H_2^+), and hydrogen cluster ions (H_3^+), with each species comprising ground states and various excited states. Thousands of interactions exist among these species, such as elastic collisions, excitation, ionization, dissociation, and recombination. Therefore, it is essential to select the dominant reaction processes for investigation. The main reaction processes in hydrogen plasma are summarized in Table 1. The ones most relevant to H_3^+ are given below: (1) composition to form H_3^+, (3) dissociation to H, (4) dissociation to H_2 and H, (5) dissociation to H and H^+.

The global model treats the plasma density and energy parameters within the discharge chamber as spatially uniform. Owing to its advantages such as low computational cost and ease of convergence, the global model has been widely used in studies of various types of plasma sources.[25–30] Based on these advantages, the global model is well suited for investigating the production mechanism of H_3^+.

Table 1. Main reaction processes in hydrogen plasma.

No.	Reaction	Type	No.	Reaction	Type
(1)	$e+H_2 \rightarrow 2e+H_2^+$	Ionization	(7)	$e+H_2 \rightarrow e+2H$	Dissociation
(2)	$H_2+H_2^+ \rightarrow H_3^+ +H$	Composition	(8)	$e+H_2 \rightarrow 2e+H+H^+$	Ionization
(3)	$e+H_3^+ \rightarrow 3H$	Dissociation	(9)	$e+H \rightarrow 2e+H^+$	Ionization
(4)	$e+H_3^+ \rightarrow H_2+H$	Recombination	(1)	$e+H_2^+ \rightarrow 2H$	Dissociation
(5)	$e+H_3^+ \rightarrow 2H+H^+ +e$	Dissociation	(11)	$e+H_2^+ \rightarrow H^+ +H+e$	Dissociation
(6)	$e+H_2 \rightarrow e+H+H$	Dissociation	(12)	$e+H_2^+ \rightarrow 2H^+ +2e$	Dissociation

Figure 1 presents the cross sections as a function of energy for selected reaction processes in hydrogen plasma. For reactions involving electrons, the horizontal axis represents the electron energy. For the H_3^+ formation reaction $H_2+ H_2^+ \rightarrow H_3^+ + H$, the horizontal axis represents the particle with higher energy, which is typically H_2^+.

The global model consists of a set of particle number density equations and particle energy equations. The number density equations can be expressed as

$$\frac{\mathrm{d}n_i}{\mathrm{d}t} = \sum n_j n_k \alpha_l - \frac{n_i}{\tau_i}, \tag{1}$$

where τ denotes the particle confinement time, and α_l represents the reaction rate of the l-th reaction, which is determined by the energies of the reacting particles. When the reaction process is dominated by electrons, the reaction rate is expressed as

$$\alpha_l = \frac{4}{\pi^{0.5}u^3}\int_{v_{\mathrm{th}}}^{\infty} v_{\mathrm{e}}^2 \sigma(E_{\mathrm{e}}) \exp(-v_{\mathrm{e}}^2/u^2)\,\mathrm{d}v_{\mathrm{e}}. \tag{2}$$

When the reaction process is dominated by ions, the reaction rate is expressed as

$$\alpha_l = \frac{1}{\pi^{0.5}uv}\int_{v_{\mathrm{th}}}^{\infty} v_{\mathrm{r}}^2 \sigma(E_{\mathrm{r}}) \left\{ \exp\left[-(v_{\mathrm{r}}-v)^2/u^2\right] - \exp\left[-(v_{\mathrm{r}}+v)^2/u^2\right] \right\} \mathrm{d}v_{\mathrm{r}}. \tag{3}$$

The particle energy equations can be expressed as

$$\frac{\mathrm{d}E_i}{\mathrm{d}t} = P_{\mathrm{i}i} + P_{\mathrm{d}i} + P_{\mathrm{c}i} - \frac{E_i}{\tau_i}, \tag{4}$$

where P_{ij}, P_{dj}, P_{cj} are power variations caused by ionization, dissociation and composition, respectively. E_i/τ_i is the energy lost due to particle loss.

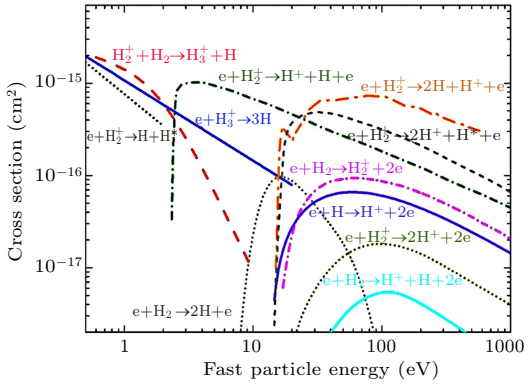


Fig. 1. Cross sections of the main processes in hydrogen plasma.[31]

In addition to the above set of equations, the charge conservation equation is also required:

$$n_e = n_{i1} + n_{i2} + n_{i3}. \tag{5}$$

By solving the above equations, the temporal evolution of the number density of each particle species during the initial establishment of the plasma can be obtained, thereby elucidating the H_3^+ production mechanisms.

2.2. Experimental setup

Figure 2(a) shows a photograph of the MMDIS source body assembled with its extraction system. The total weight is 7.6 kg and the source body is about 2.1 kg. This ion source has been well miniaturized such that the diameter of the inner discharge chamber is only 24 mm. Figure 2(b) presents a photograph of the MMDIS installed on the ion source test bench. Detailed parameters of the ion source body and the test bench are described comprehensively in Ref. [24].

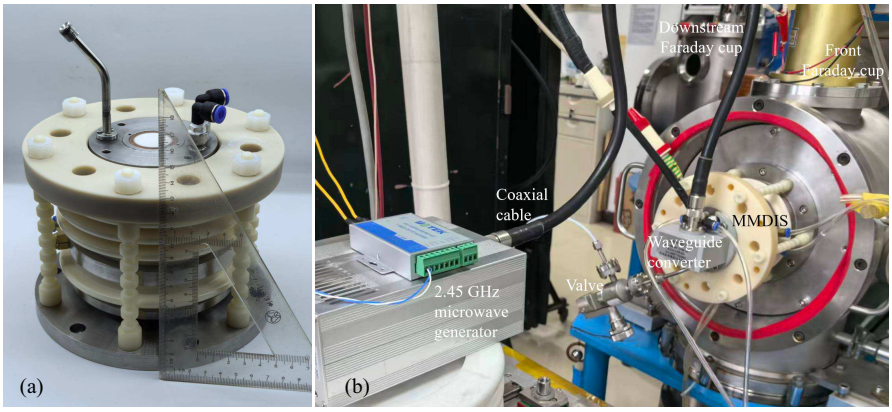


Fig. 2. Photos of (a) MMDIS and (b) MMDIS installed on the test bench.

During the experiments, the ion source was operated in DC mode, with the microwave power ranging from 50 W to 200 W and the gas pressure in the vacuum chamber behind the ion source varying from 7×10^{-4} Pa to 4×10^{-3} Pa. The extraction voltage was maintained at 30 kV.

3. Simulations and experimental results

3.1. Simulation results

The simulated operating condition was a gas pressure of 3×10^{-3} Pa and a microwave power of 100 W. Figure 3 shows the temporal evolution of the particle number densities during the initial discharge stage under this condition. Before 1.2 μs, the H_2^+ number density increased faster than that of H_3^+. Before 3.8 μs, the number density of H_2^+ was higher than that of H_3^+. After 3.8 μs, the H_3^+ number density surpassed that of H_2^+ and continued to increase, becoming the dominant species among the three ions. This indicates that H_2^+ is the ion formed earliest during the initial discharge stage. For the H_3^+ formation reaction $H_2 + H_2^+ \rightarrow H_3^+ + H$, a sufficient quantity of H_2^+ is required to produce H_3^+ rapidly and abundantly, which accounts for the higher generation rate of H_2^+ compared to H_3^+ in the early phase of the reaction. To obtain an H_3^+ - dominated beam, an adequate supply of H_2 is also necessary, along with a reduction in the average electron temperature to suppress the generation rate of H_2^+.

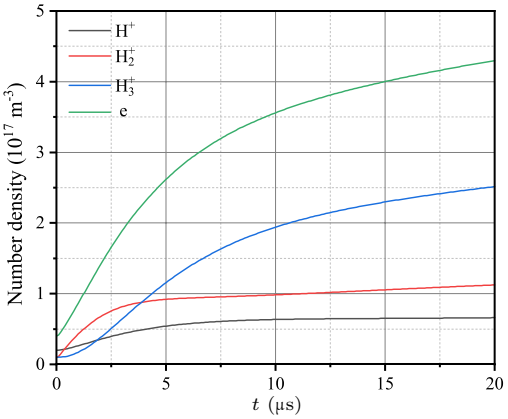


Fig. 3. Transition variation diagram of particle number density in the initial state of discharge.

Figure 4(a) shows the variation in the reaction rate of $H_2+ H_2^+ \rightarrow H_3^+ + H$ at 2.0×10^{-3} Pa under different microwave powers. The figure indicates that as the power increases from 60 W to 80 W, the reaction rate gradually rises. However, when the power reaches 90 W, the reaction rate drops below that observed at 80 W, 20 μs. This suggests that excessively high microwave power inhibits the reaction $H_2+ H_2^+ \rightarrow H_3^+ + H$, thereby hindering the formation of H_3^+. Figure 4(b) shows the variation in the reaction rate of $H_2+ H_2^+ \rightarrow H_3^+ + H$ at 90 W under different gas pressure. It can be seen that as the gas pressure increases, the reaction rate gradually rises, promoting the formation of H_3^+.

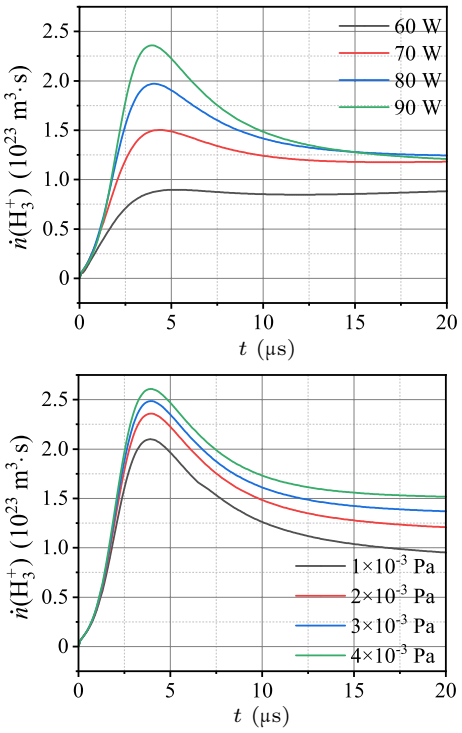


Fig. 4. (a) Effect of microwave power on reaction $H_2+ H_2^+ \rightarrow H_3^+ + H$. (b) Effect of gas pressure on reaction $H_2+ H_2^+ \rightarrow H_3^+ + H$.

3.2. Experimental results

Figure 5 shows the H_3^+ beam currents under different microwave powers and gas pressures. As shown in the figure, at a given gas pressure, the H_3^+ beam current exhibits a non-monotonic dependence on microwave power, first increasing and then decreasing. When the microwave power is relatively low, the plasma discharge is not fully established. Increasing the microwave power leads to a rapid increase in the plasma density, which also raises the H_3^+ ion density, thereby enhancing the extracted H_3^+ beam current. With a further increase in microwave power, the growth rate of the plasma density slows down, while the electron temperature rises, promoting reactions such as $e + H_3^+ \rightarrow 3H$, $e + H_3^+ \rightarrow H_2+ H$, and $e + H_3^+ \rightarrow 2H + H^+ + e$. These reactions consume H_3^+, resulting in a gradual decline in the H_3^+ beam current as the power increases. This phenomenon is consistent with that shown in Fig. 4(a).

For a given microwave power, the H_3^+ beam current also exhibits a non-monotonic trend of first increasing and then decreasing with increasing gas pressure. When the gas pressure is too low, a dense plasma cannot be formed, and the density of H_2 is insufficient, which is unfavorable for the reaction $H_2+ H_2^+ \rightarrow H_3^+ + H$. Increasing the gas pressure leads to a higher plasma density and a higher H_2 density, resulting in an increase in the H_3^+ beam current. However, a further increase in gas pressure reduces the average electron temperature, which impedes the ionization of neutral particles and lowers the plasma density, thereby causing the H_3^+ beam current to decrease.

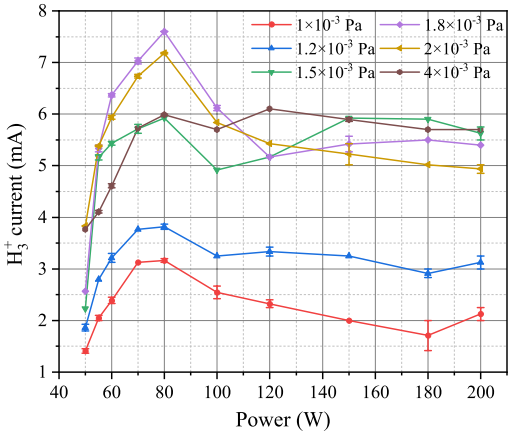


Fig. 5. H_3^+ beam current measured on the downstream Faraday cup under different microwave powers at different gas pressures.

Therefore, to generate a high-current H_3^+ beam, an optimal microwave power and gas pressure are required. At 1.8×10^{-3} Pa and 80 W, a maximum H_3^+ beam current of 7.6 mA was achieved.

Figure 6 shows the H_3^+ ion fraction under different microwave powers and gas pressures. As shown in the figure, at a given gas pressure, the H_3^+ ion fraction decreases gradually with increasing microwave power. With increasing power, the plasma density rises, significantly enhancing the production of H^+ and H_2^+, both of which are formed via electron-impact ionization. The increase in plasma density leads to rapid growth in the densities of H^+ and H_2^+, thereby reducing the fraction of H_3^+. At a fixed microwave power, plasma density does not increase monotonically with operating pressure but instead peaks at an optimal pressure and then declines. Correspondingly, the beam currents of H^+, H_2^+, and H_3^+ decrease beyond this optimum pressure. According to the reaction $H_2+ H_2^+ \rightarrow H_3^+ + H$, elevated pressure raises the H_2 density, which promotes H_3^+ formation while suppressing the generation of H^+ and H_2^+. As a result, the beam currents of H^+ and H_2^+ drop more rapidly, leading to an increased fraction of H_3^+. This phenomenon is consistent with that shown in Fig. 4(b). The maximum H_3^+ fraction of 68.5% was obtained at 50 W and

4×10^{-3} Pa. It is worth noting that the H_3^+ fraction will continue to increase with increasing gas pressure, but the H_3^+ current will decrease, which is inconsistent with the objective of this work to obtain a high H_3^+ beam current. Therefore, the gas pressure will no longer be increased in this experiment.

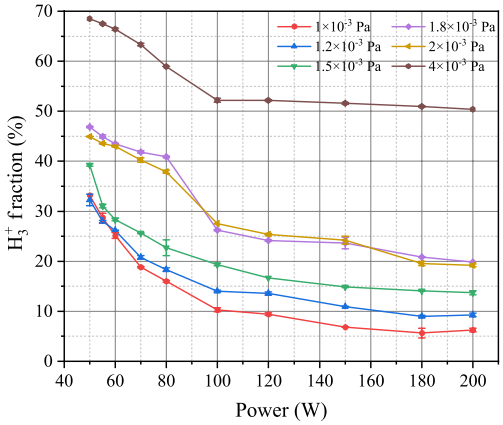


Fig. 6. H_3^+ fraction under different microwave powers and gas pressures.

During the experiment, the beam currents of H^+ and H_2^+ were also measured. For H^+, the maximum beam current was 19.7 mA and the maximum fraction was 48.7%; for H_2^+, the corresponding values were 24.0 mA and 69.8%, respectively. For each operating condition defined by a given gas pressure and microwave power, there exists a dominant ion species, which accounts for the highest fraction among H^+, H_2^+ and H_3^+. The beam currents of the dominant ions are represented in the diagram, as shown in Fig. 7. In this figure, the red region denotes the H^+-dominant regime, the blue region denotes the H_2^+-dominant regime, and the green region denotes the H_3^+-dominant regime. The color intensity reflects the magnitude of the beam current. It can be seen that, for H_3^+, low power and high gas pressure favor its dominance, and a maximum H_3^+ beam current of 7.6 mA was measured experimentally and the maximum fraction of H_2^+ was 69.8%. Under high gas pressure, increasing the power does not significantly enhance the H_3^+ beam current. Therefore, to generate a high-current H_3^+ beam, a gas pressure of 1.8×10^{-3} Pa and a microwave power of 80 W should be selected. Compared to the pressure and power values at which the H^+ or H_2^+ beam current peaks, the pressure corresponding to the maximum H_3^+ beam current is higher, and the power is at a moderately low level.

Investigations on H^+ and H_2^+ were carried out simultaneously. For H^+, moderate gas pressure and high power facilitate its dominance, and a maximum H^+ beam current of 19.7 mA with a fraction of 48.7% was obtained experimentally. For H_2^+, low gas pressure favors its dominance, with a maximum H_2^+ beam current of 24.0 mA measured and the maximum fraction of H_2^+ was 69.8%. Notably, these results are superior to those reported in Ref. [24], which were achieved at PKU several months prior. The trend shown in the ternary diagram is consistent with that in Ref. [32]. Moreover, this work advances the previously qualitative diagram to a quantitative one, which is of greater utility for the design and commissioning of hydrogen ion sources.

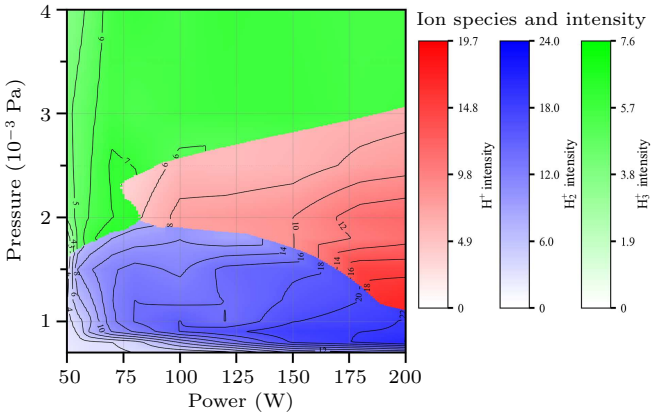


Fig. 7. Ternary diagram of hydrogen plasma in MMDIS.

4. Conclusion

The H_3^+ ion beam is of considerable interest in a wide range of fields, making a high-current H_3^+ ion source highly desirable. In this work, the generation mechanism of H_3^+ was investigated. Experimentally, a 7.6 mA H_3^+ ion beam was generated, and the maximum H_3^+ fraction of 68.5% was found in the DC mode by a miniaturized permanent magnet 2.45 GHz MDIS. In addition, the maximum pure H_2^+ beam was 24 mA, higher than the published value in 2025, and a 19.7 mA H^+ beam was also obtained. The results demonstrate that the generation of a high-current H_3^+ beam requires high gas pressure and low microwave power conditions. Based on the experimental results, a quantitative ion ternary diagram was constructed, providing important theoretical guidance for the design and optimization of ion sources. These findings will serve as a valuable reference for applications requiring high-current H_3^+ beams.

Acknowledgements

Project supported by the National Natural Science Foundation of China (Grant No. 11975036). We appreciate the support from the State Key Laboratory of Nuclear Physics and Technology at PKU.

References

[1] Calabretta L, Maggiore M, Piazza L, Rifuggiato D andCalanna A 2010 *Proceedings of Cyclotron'10 Conference*, Lanzhou, China, Sept. 7
[2] Alonso J R, Calabretta L, Campo D, Celona L, Conrad J, Martinez R G, Johnson R, Labrecque F, Toups M H, Winklehner D and Winslow L 2014 *Rev. Sci. Instrum.* **85** 02A742
[3] Winklehner D, Conrad J M, Smolsky J and Waites L H 2021 *Rev. Sci. Instrum.* **92** 123301
[4] Winklehner D, Engebretson S, Moon J, Villarreal J, Weigel P, Winkler E and Landon P 2025 *J. Phys. G: Nucl. Part. Phys.* **52** 115001
[5] Kolano A, Adelmann A, Barlow R and Baumgarten C 2018 *Nucl. Instrum. Meth. A* **54** 885

[6] Alonso J R, Barlow R, Conrad J M and Waites L H 2019 *Nat. Rev. Phys.* **533** 1

[7] Bylinskii Y, Baartman R, Dirksen P, Rao Y N and Verzilov V 2018 *Proceedings of the 9th International Particle Accelerator Conference*, Vancouver, Canada, pp. 1159–1162

[8] Alonso J, Axani S, Calabretta L, Campo D, Celona L, Conrad J M, Day A, Castro G, Labrecque F and Winklehner D 2015 *J. Instrum.* **10** T10003

[9] Winklehner D, Axani S, Bedard P, Conrad J, Corona J, Hartwell F,Smolsky J, Tripathee A, Waites L, Weigel P, Wester T and Yampolskaya M 2018 *AIP Conf. Proc.* **2011** 030002

[10] Rao Y N, Zhang L, Baartman R, Bylinskii Y, Koay H and Planche T 2023 *ICFA Beam Dynamics Newsletter*

[11] Koay H W 2023 *J. Instrum.* **18** P03027

[12] Yenen O, Wiese L M, Calabrese D and Jaecks D H 1990 *Phys. Rev. A* **42** 324

[13] Oka T 2012 *Philos. Trans. R. Soc. A* **370** 4991

[14] Miller S, Tennyson J, Geballe T R and Stallard T 2020 *Rev. Mod. Phys.* **92** 035003

[15] Leung S Y, Tolk N H, Heiland W, Tully J C, Kraus J S and Hill P 1978 *Phys. Rev. A* **18** 447

[16] Moak C D, Banta H E, Thurston J N, Johnson J W and King R F 1959 *Rev. Sci. Instrum.* **30** 694

[17] Oks E M and Shandrikov M V 2016 *Rev. Sci. Instrum.* **87** 02B703

[18] Joshi N, Droba M, Meusel O and Ratzinger U 2009 *Nucl. Instrum. Meth. A* **606** 310

[19] Xu Y, Peng S, Ren H, Zhang A, Zhang T, Zhang J, Wen J, Wu W, Guo Z and Chen J 2017 *Chin. Phys. B* **26** 085203

[20] Wu W, Peng S, Ma T, Ren H, Zhang J, Zhang T, Jiang Y, Li K, Xu Y, Zhang A, Wen J, Guo Z and Chen J 2019 *Rev. Sci. Instrum.* **90** 101501

[21] Xu Y, Peng S, Ren H, Zhao J, Chen J, Zhang A, Zhang T, Guo Z and Chen J 2013 *Rev. Sci. Instrum.* **85** 02A943

[22] Wen J, Peng S, Ren H, Zhang T, Zhang J, Wu W, Sun J, Guo Z and Chen J 2018 *Chin. Phys. B* **27** 055204

[23] Peng S, Ma T, Wu W, Cui B, Zhang A, Jiang Y, Guo Z and Chen J 2023 *Radiat. Detect. Technol. Methods* **7** 545

[24] Cui B, Peng S, Zhu J, Dong Y, Guo Z and Chen J 2025 *Chin. Phys. B* **34** 085203

[25] Chan C, Burrell C and Cooper W 1983 *J. Appl. Phys.* **54** 6119

[26] Lieberman M and Ashida S 1996 *Plasma Sources Sci. Technol.* **5** 145

[27] Wauters T, Lyssoivan A, Douai D, Marchuk O, Wunderlich D, Koch R, Sergienko G, Oost G and Schoor M 2011 *Plasma Phys. Contr. Fusion* **53** 125003

[28] Little J and Kelly C 2020 *Phys. Plasmas* **27** 11

[29] Skalyga V, Zorin V, Izotov I, Razin S, Sidorov A and Bohanov A 2006 *Plasma Sources Sci. Technol.* **15** 727

[30] Samuell C M and Corr C S 2016 *Plasma Sources Sci. Technol.* **25** 015014

[31] Janev R K, Langer W D and Douglass E Jr Springer Science & Business Media, 1987

[32] Peng S, Wu W, Ren H, Zhang J, Xu Y, Zhang A, Zhang T, Ma T, Jiang Y, Sun J, Wen J, Guo Z and Chen J 2019 *Rev. Sci. Instrum.* **90** 123305